Journal of Applied Biological Sciences 6 (3): 45-55, 2012
ISSN: 1307-1130, E-ISSN: 2146-0108, www.nobel.gen.tr

Multi-Spectroscopic Investigation of the Interactions between Cholesterol and Human Serum Albumin

M. M. Abu TEIR* J. GHITHAN S. DARWISH M. M. ABU-HADID

Al-Quds University, P.O.Box 72851, JERUSALEM

*Corresponding Author
e-mail: abuteir@science.alquds.edu

Received: April 23, 2012
Accepted: May 28, 2012

Abstract

The interaction between cholesterol and human serum albumin has been investigated. The basic binding interaction was studied by UV-absorption and fluorescence spectroscopy. From spectral analysis cholesterol showed a strong ability to quench the intrinsic fluorescence of HSA through a static quenching mechanism. The binding constant (k) is estimated to be $K=0.214 \times 10^4\ M^{-1}$ at 293 K. FTIR spectroscopy with Fourier self-deconvolution technique was used to determine the protein secondary structure and cholesterol binding mechanisms. The observed spectral changes indicate a higher percentage of H-bonding between cholesterol and a-helix (secondary structure motif in HSA) compared to the percentage of H-bonding between cholesterol and b-sheets (secondary structure motif in HSA).

Keywords: cholesterol; amide I, amide II, amid III ; binding mode; binding constant; protein secondary structure; Fourier transform IR; UV–spectroscopy, Fluorescence spectroscopy.

INTRODUCTION

Cholesterol is an extremely important biological molecule being an essential component of cell membrane as well as a precursor for the synthesis of a number of essential vitamins, steroid hormones and bile acids, its chemical structure is shown in Figure 1 [1].

Human serum albumin (HSA) is the most abundant carrier protein of the body with a high affinity for a wide range of metabolites and drugs. The most important physiological role of HSA is to carry such solutes in the blood stream and then deliver them to the target organs, as well as to maintain the pH and osmotic pressure of plasma [2].The molecular interactions between HSA and many compounds have been investigated [3,4,5]. It has been recently proved that serum albumin plays a decisive role in the transport and disposition of a variety of endogenous and exogenous compound such as fatty acids, hormones, bilirubin, drugs… [6]. The distribution and metabolism of many biologically active compounds in the body whether drugs or natural products are correlated with their affinities toward serum albumin. Thus, the study of the interaction of such molecules with albumin is of imperative and fundamental importance [7]. Extensive studies on different aspects of drug–HSA interactions are still in progress because of the clinical significance of the process [8].

Numerous analytical techniques are used for ligand protein binding studies and they are continuously extending our knowledge about the complex mechanisms involved in the drug–HSA binding process[9].

In this work, we have investigated the interactions of cholesterol with HSA by means of FTIR, UV/VIS, and fluorescence spectrometers.

This work will be limited to the mid-range infrared, which covers the frequency range from 400 to 4000 cm^{-1}. This wavelength region includes bands that arise from three conformational sensitive vibrations within the peptide backbone (Amides I, II and III). Among them amide I is the most widely used band because it can provide information on secondary structure composition and structural stability [12,13,14].

Infrared spectroscopy provides measurements of molecular vibrations due to the specific absorption of infrared radiation by chemical bonds. It is known that the form and frequency of the Amide I band, which is assigned to the C=O stretching vibration within the peptide bonds is very characteristic for the structure of the studied protein . From the bands of secondary structures, components of α-helix, β-sheets peaks can be derived and the analysis of these bands allows us to elucidate the conformational changes with high sensitivity [10,11].

Other spectroscopy techniques are usually used to study the interaction of many small molecules to proteins, fluorescence and UV spectroscopy are commonly used because of their high sensitivity, rapidity and ease of implementation [15,16,17].

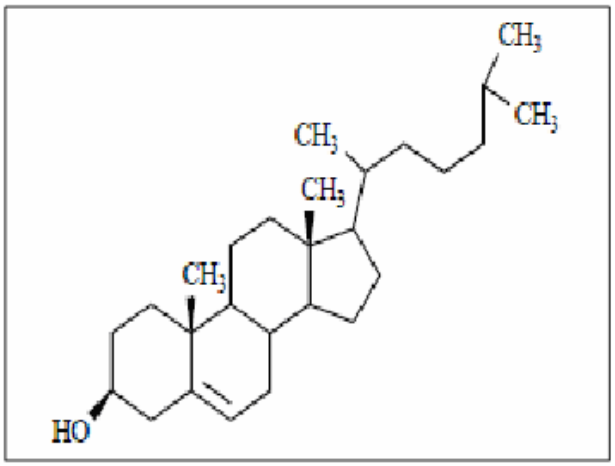

Figure 1. Chemical structure of cholesterol.

MATERIALS AND METHODS

HSA (fatty acid free), and Cholesterol in solid form were purchased from Sigma Aldrich chemical company and used without further purifications.

The data was taken using thin films samples for FTIR measurements and solution samples for UV/VIS and fluorescence measurements.

Preparation of HSA stock solution

HSA was dissolved in phosphate buffer saline pH 7.4 (80mg/ml) .

Preparation of Cholesterol stock solution

Cholesterol was dissolve in phosphate buffer saline (0.0009373g/ml), the solution was put in ultrasonic water path (SIBATA AU-3T) for six hours to ensure that all the amount of cholesterol was dissolved completely.

HSA-Cholesterol solutions

The final concentration of HSA-Cholesterol solutions were prepared by mixing equal volume of HSA solution with fixed concentration and Cholesterol solution with different concentrations. HSA concentration in all samples is 40mg/ml. However, the concentration of Cholesterol in the final protein cholesterol mixtures were decreased such that the molecular ratio (HSA:Cholesterol) started at 10:18, 10:14, 10:10, 10:6, and ended at 10:2.

Thin film preparations

Silicon windows (NICODOM Ltd) were used as spectroscopic cell windows. The optical transmission is high with little or no distortion of the transmitted signal. The 100% line of a NICODOM silicon window shows that the silicon bands in the Mid Infra Red (MIR) region do not exhibit total absorption and can be easily subtracted.

50µl of each sample of HSA-Cholesterol mixture were placed on a silicon window and incubated at temperature 25 ^{0}C to evaporate the solvent. To obtain a transparent thin film on the silicon windows, all the samples were prepared at room tempreture.

UV/VIS spectrophotometer (NanoDrop ND-1000)

The absorption spectra were obtained by the use of a NanoDrop ND-1000 spectrophotometer. It is used to measure the spectrum of the samples in the range between 220-750nm, with high accuracy and reproducibility.

Fluorospectrometer (NanoDrop 3300)

The fluorescence measurements were performed by a NanoDrop ND-3300 Fluorospectrometer at 25 ^{o}C. The excitation source comes from one of three solid-state light emitting diodes (LED's). The excitation source options include: UV LED with maximum excitation 365 nm, Blue LED with excitation 470 nm, and white LED from 500 to 650nm excitation. A 2048-element CCD array detector covering 400–750 nm, is connected by an optical fiber to the optical measurement surface. The excitation is done at the wavelength of 360 nm and the maximum emission wavelength is at 439 nm.

FTIR Spectroscopy Experimental Procedures

The FTIR measurements were obtained on a Bruker IFS 66/S spectrophotometer equipped with a liquid nitrogen-cooled MCT detector and a KBr beam splitter. The spectrometer was continuously purged with dry air during measurements.

The absorption spectra were obtained in the wave number range of 400–4000 cm^{-1}. A spectrum was taken as an average of 60 scans to increase the signal to noise ratio, and the spectral resolution was at 4 cm^{-1}. The aperture used in this study was 8 mm, since we found that this aperture gives best signal to noise ratio. Baseline correction, normalization and peak areas calculations were performed for all the spectra by OPUS software. The peak positions were determined using the second derivative of the spectra.

The infrared spectra of HSA, and Cholesterol–HSA complex were obtained in the region of 1000–1800 cm^{-1}. The FTIR spectrum of free HSA was acquired by subtracting the absorption spectrum of the buffer solution from the spectrum of the protein solution. For the net interaction effect, the difference spectra {(protein and Cholesterol solution) – (protein solution)} were generated using the featureless region of the protein solution 1800-2200 cm^{-1} as an internal standard[18].

RESULT AND DISCUSSION

UV-absorption spectroscopy

Many studies have reported the effective use of UV-VIS spectroscopy to investigate the interaction of drugs with HSA[19,20,21]. The absorption spectra of cholesterol HSA solutions is displayed in Figure 2. The excitation has been done on 210 nm and the absorption is recorded at 280 nm. It is clear that the UV-VIS absorption spectrum of HSA increases with increasing the cholesterol concentration in the HSA -cholesterol mixture. Also the absorption peaks of these solutions showed moderate shifts indicating that with the increase of the cholesterol concentration, the peptide strands of HSA molecules extended more and the hydrophobicity is increased. The results indicated that an interaction occurred between cholesterol and HSA. It is clear from the spectrum in Figures 2 that pure cholesterol has little or no UV absorption which indicate that the resulted peaks are due to the interactions between cholesterol and HSA. Repeated measurements were done for all the samples and no significant differences were observed.

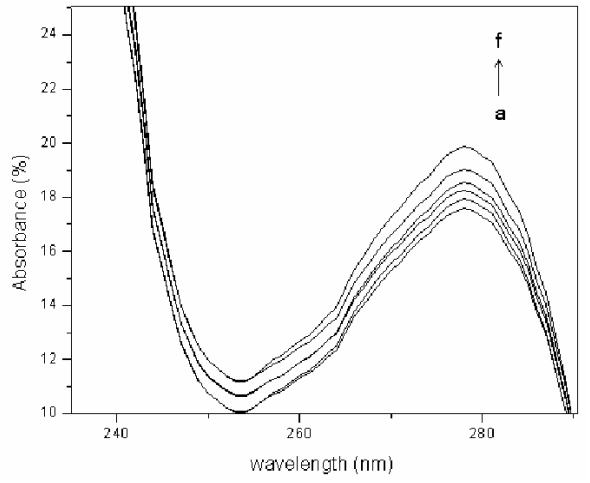

Figure 2. UV-Absorbance spectra of HSA with different contents of cholesterol (a=0:10, b=2:10, c=6:10, d=10:10, e=14:10, f=18:10).

The cholesterol - HSA complexes binding constants were determined using UV-VIS spectrophotometer according to published method[22,23,24]. By assuming that there is only one type of interaction between cholesterol and HSA in aqueous solution, leads to establish Equations. (1) and (2) as follows:

$$\text{HSA} + \text{cholesterol} \leftrightarrow \text{Cholesterol: HSA} \quad (1)$$

$$K = [\text{Cholesterol: HSA}]/[\text{Cholesterol}][\text{HSA}] \quad (2)$$

The absorption data were treated using linear double reciprocal plots based on the following equation[25]:

$$\frac{1}{A - A_0} = \frac{1}{A_\infty - A_0} + \frac{1}{K[A_\infty - A_0]} \cdot \frac{1}{L} \quad (3)$$

where A_0 corresponds to the initial absorption of protein at 280 nm in the absence of ligand, A_∞ is the final absorption of the ligated protein, and A is the recorded absorption at different Cholesterol concentrations (L). The double reciprocal plot of $1/(A - A_0)$ vs. 1/L is linear (Figure 3) and the binding constant (K) can be estimated from the ratio of the intercept to the slope to be $6.354\times10^2 M^{-1}$ for Cholesterol - HSA complexes. The value obtained is indicative of a weak cholesterol protein interaction with respect to the other drug-HSA complexes with binding constants in the range of 10^5 and 10^6 M^{-1}[26]. The reason for the low stability of the Cholesterol HSA complexes can be attributed to the presence of mainly hydrogen bonding interaction between protein accepter atoms and the cholesterol polar group(-OH) as donor or an indirect cholesterol- protein interaction through water molecules. Similar weak interactions were observed in cis- $Pt(NH_3)_2$–HSA and taxol–HSA complexes[27,28].

Fluorescence spectroscopy

Fluorescence spectroscopy is one of the most widely used spectroscopic techniques in the fields of biochemistry and molecular biophysics today [29]. The autofluorescence of HSA comes from the tryptophan, tyrosine and phenylalanine residues. Actually, the intrinsic fluorescence of HSA is almost contributed by tryptophan alone, because phenylalanine has a very low quantum yield and the fluorescence of tyrosine is almost totally quenched if it is ionized or near an amino group, a carboxyl group or a tryptophan [30].

In our investigation of HSA- cholesterol mixtures we have done the excitation at 360nm wavelength and observed the emission at 439nm wavelength. The fluorescence sensor is based on intramolecular charge transfer (ICT), which is highly sensitive to the polarity of microenvironment. Therefore, it is expected to act as fluorescent probe for some biochemical system like proteins [31].

The fluorescence quenching spectra of HSA at various contents of Cholesterol is shown in Figure 4. Obviously the fluorescence intensity of HSA gradually decreased while the peak position shows little or no change upon increasing the concentration of cholesterol, suggesting the binding of cholesterol to HSA. Under the same condition, no fluorescence of cholesterol was observed. Which indicates that cholesterol could quench the autofluorescence of HSA and that the interaction between cholesterol and HSA indeed existed leading to a change in the microenvironment around the tryptophan residue and further exposure of tryptophan residue to the polar solvent [32,33,34]. Fluorescence quenching refers to any process, which decreases the fluorescence intensity of a sample [25]. Variety of molecular interactions can result in quenching, these include excited-state reactions, molecular rearrangements,

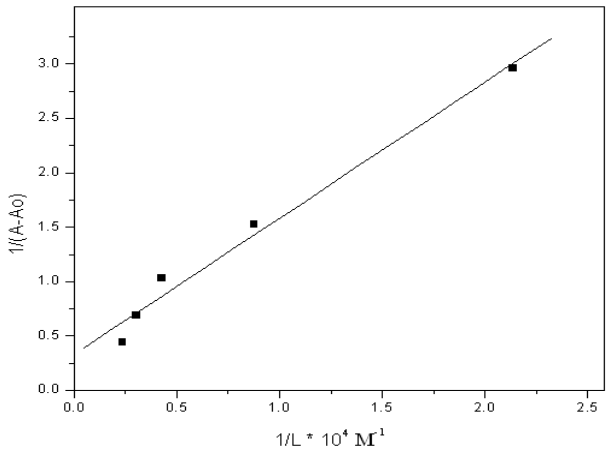

Figure 3. The plot of 1/(A-Ao) vs 1/L for HSA with different concentrations of cholesterol.

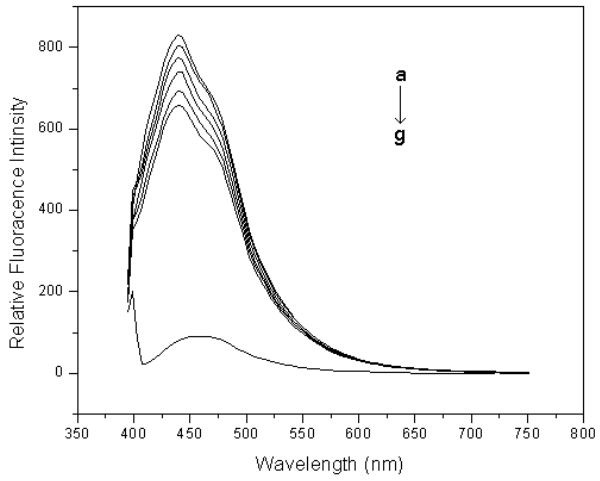

Figure 4. Fluorescence emission spectra of HSA in the absence and presence of cholesterol in these ratios (cholesterol : HSA a=0:10, b=2:10, c=6:10, d=10:10, e=14:10, f=18:10, g=free cholesterol)

energy transfer, ground-state complex formation, and collisional quenching [36]. Fluorescence quenching can be induced by different mechanisms, usually classified into dynamic and static quenching [35].

As mentioned before, assuming dynamic quenching is dominant between cholesterol and HSA, then the decrease in intensity is described by the well-known Stern-Volmer equation:

$$\frac{F_0}{F} = 1 + K_q\tau_0(L) = 1 + K_{sv}(L) \quad (4)$$

In this expression F and F_0 are the fluorescence intensities with and without quencher, K_{sv} is the Stern-Volmer quenching constant, K_q is the bimolecular quenching constant, τ_0 is the unquenched lifetime, and [Q] is the quencher concentration. The Stern-Volmer quenching constant K indicates the sensitivity of the fluorophore to a quencher.

Linear curves were plotted according to the Stern– Volmer equation as shown in figure 5 for cholesterol - HSA mixtures. The Stern–Volmer quenching constant K_{sv} was obtained by the slope of the curves obtained in figures 5 and its value equals 6.26×10^2 L $mol^{-1}$for Cholesterol - HSA mixtures. Obviously from equation 4 the value of $K_{sv}=K_q\,\tau_0$, from which we can calculate the value of K_q using the fluorescence life time of 10^{-8} s for HSA [36,37] the obtained values of K_q equals 6.2×10^{10} L $mol^{-1}$for cholesterol - HSA mixtures. Which is larger than the maximum dynamic quenching constant for various quenchers with biopolymer (2×10^{10} L mol^{-1} s^{-1})[38,39].

So, this shows that the quenching is not initiated by dynamic collision but from formation of a complex, so static quenching is dominant [35,40] When static equilibrium is dominant one can use the modified Stern-Volmer equation [41]:

$$\frac{1}{F_0 - F} = \frac{1}{F_0K(L)} + \frac{1}{F_0} \quad (5)$$

Where K is the binding constant of cholesterol with HSA, and can be calculated by plotting $1/(F_0\text{-}F)$ vs 1/L, figure 6. The value of K equals the ratio of the intercept to the slope. The obtained values of K equals $K=0.214\times10^4$ M^{-1} for Cholesterol - HSA mixtures from figure 6 which agrees well with the value obtained earlier by UV spectroscopy and supports

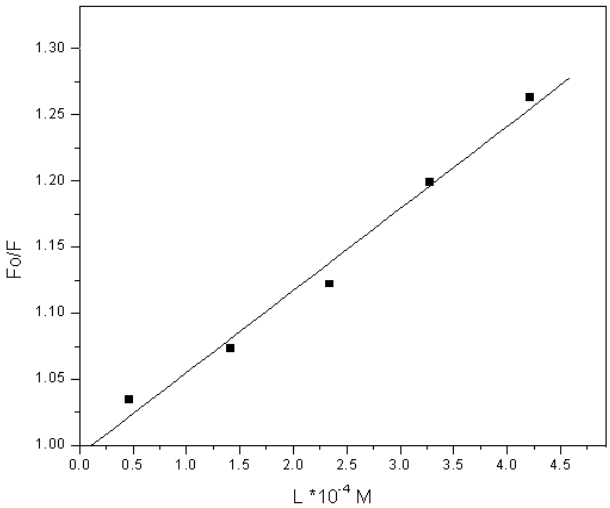

Figure 5. The Stern-Volmer plot for cholesterol- HSA complexes.

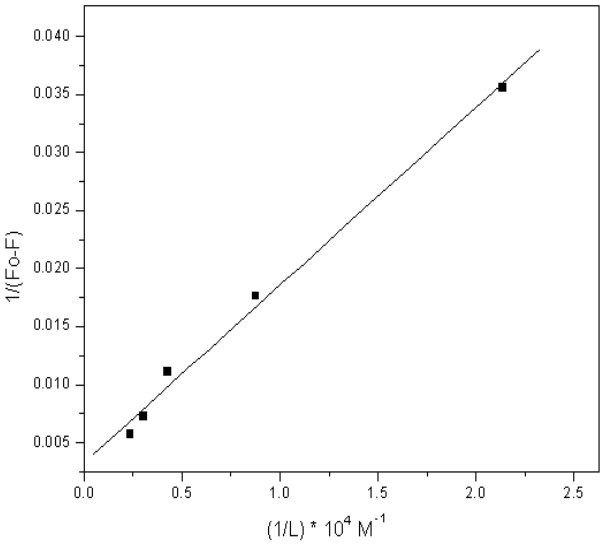

Figure 6. The plot of 1/(Fo-F) vs $(1/L)\times10^4$ for cholesterol- HSA complexes.

the effective role of static quenching. The highly effective quenching constant in this case has lead to a lower value of binding constant between the cholesterol and HSA due to an effective hydrogen bonding [10,11]. The acting forces between a small molecule substance and macromolecule mainly include hydrogen bond, van der Waals force, electrostatic force and hydrophobic interaction force. It was more likely that hydrophobic, electrostatic interactions and the hydrogen bonds were involved in the binding process. However, cholesterol might be largely unionized under the experimental conditions, as expected from its structure. Hence, electrostatic interaction could be precluded from the binding process. Thus, the binding of cholesterol to HSA includes the hydrophobic interaction and hydrogen bonds[42].

FT-IR Spectroscopy

FT-IR spectroscopy is a powerful technique for the study of hydrogen bonding[43], and has been identified as one of the few techniques that is established in the determination of protein secondary structure at different physiological systems [44,45]. The information on the secondary structure of proteins arises from the amide bands which result from the vibrations of the peptide groups of proteins. When small molecules bind to a globular protein like HSA, changes in hydrogen bonding which is involved in the peptide linkages would occurs, resulting in changes in the vibrational frequency of the different amide modes [46,47].

The modes most widely used in protein structural studies are amide I, amide II and amide III. Amide I band ranging from 1600 to 1700 cm^{-1} and arises principally from the C=O stretching [48] and has been widely accepted to be used for two purposes [49]. Amide II band is primarily N-H bending with a contribution from C-N stretching vibrations, amide II ranging from 1480 to 1600 cm^{-1}. Amide III band ranging from 1220 to 1330 cm^{-1} which is due to the C-N stretching mode coupled to the in-plane N-H bending mode.

The second derivative of free HSA is shown in figures 7A and 7B, where the spectra is dominated by absorbance bands of amide I and amide II at peak positions 1656cm $^{-1}$ and 1543cm^{1}, respectively. Figure 7B, shows the spectrum of cholesterol-

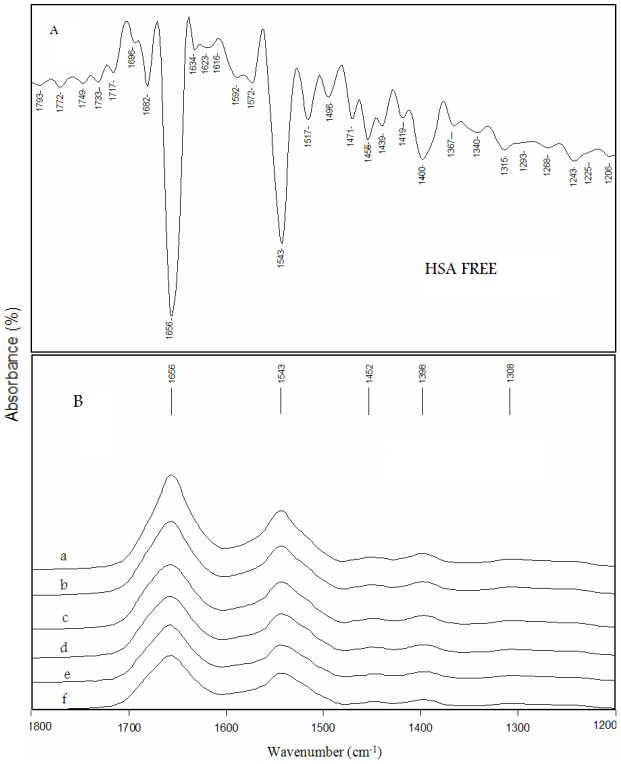

Figure 7. A: The spectra of HSA free (second derivative) And B: (a, b, c, d, e, f) Cholesterol-HSA with ratios (0:10, 2:10, 6:10, 10:10, 14:10, 18:10).

HSA mixtures with fixed HSA concentration and different cholesterol concentration. It is obviously seen as cholesterol content of the mixtures is increased, the intensities of amide I, amide II and amide III are decreased. The reduction in the intensity of the three amide bands is related to the cholesterol-HSA interactions.

Tables 1 lists the peak positions and their respective shifts of HSA with different contents of cholesterol. These peak position shifts for amid I band came to be as follows: 1616 to 1614cm-1, 1623 to 1628cm-1, 1656 to 1657cm-1, 1682 to 1681cm-1, and 1696 to 1692cm-1. Also a peak at 1634cm-1 has disappeared after the interaction of cholesterol with HSA. In amide II the peak positions have shifted as follows: 1496 to 1497cm-1, 1517 to 1515cm-1, 1543 to 1549cm-1, 1572 to1569cm-1, and 1592 to 1596cm-1. In addition a new peak at 1584cm-1 appeared after the interaction of cholesterol with HSA. In amide III region the peak positions have been also shifted in the following order: 1268 to 1269cm-1, and 1293 to 1296cm-1, and 1315 to 1313cm^{-1}. In addition, a peak at 1243cm^{-1} remains unchanged after the interaction of cholesterol with HAS and a peak at 1225cm-1 has disappeared after the interaction of cholesterol with HSA.

The shifts in peak positions and shape of HSA amides after cholesterol mixing with HSA come from the changes in protein secondary structure. The minor changes in peak positions can be attributed to the effect of the newly imposed H-bonding between the cholesterol molecules and the protein. It is suggested that, the shift to a higher frequency for the major peak in amide I region (1623–1628cm-1) for cholesterol- HSA mixtures came as a result of hydrogen bonding stabilizing the C–N bond to assume partial double bond character due to electrons flow from the C=O to the C–N bond[50].

Table 1. Band assignment in the absorbance spectra of HSA with different cholesterol contents for amide I, amide II, and amide III regions

Bands	HSA free	Chol:HSA 2:10	Chol:HSA 6:10	Chol:HSA 10:10	Chol:HSA 14:10	Chol:HSA 18:10
Amide I (1700-1600)	1616	1613	1611	1612	1616	1614
	1623	1626	1626	1627	1627	1628
	1634					
	1656	1655	1657	1657	1658	1657
	1682	1682	1681	1681	1681	1681
	1696	1693	1692	1693	1693	1692
Amide II (1600-1480)	1496	1497	1497	1496	1497	1497
	1517	1515	1514	1514	1515	1515
	1543	1547	1548	1548	1549	1549
	1572	1571	1570	1570	1570	1569
		1582	1582	1582	1589	1584
	1592	1595	1595	1595	1595	1596
Amide III (1330-1220)	1225					
	1243	1243	1243	1243	1243	1243
	1268	1270	1269	1269	1268	1269
	1293	1298	1298	1297	1297	1296
	1315	1314	1313	1315	1314	1313

The difference spectra for [(HSA + cholesterol) - (HSA)] were obtained in order to monitor the intensity variations of these vibrations; the results are shown in Figures 8, and 9. Figure 8 shows FT-IR spectra (top two curves) and difference spectra of HSA and its mixtures with different cholesterol contents in amide I and amide II regions and figure 9 shows FT-IR spectra (top two curves) and difference spectra of HSA and its mixtures with different cholesterol concentrations in amide III region. In amide I region clearly there is a strong negative feature at 1654cm^{-1} with a little shift in its position, and in amide II region one negative feature was also observed at 1543cm^{-1} also with a little shift in its position (figure 8). For amide III region two negative feature was observed at 1245cm^{-1} and at 1311cm^{-1} with a little shift in their positions as cholesterol contents was increased, another weak negative feature was observed at

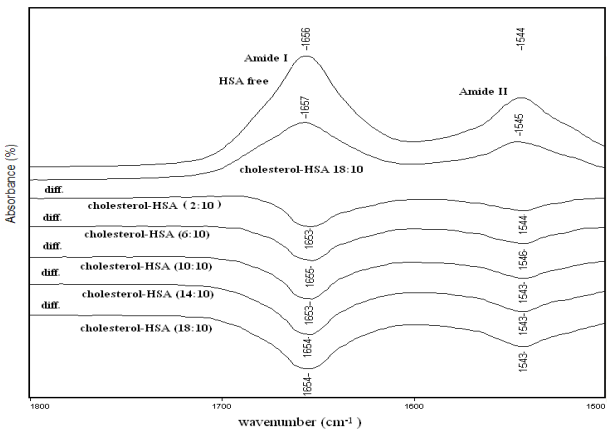

Figure 8. FT-IR spectra (top two curves) and difference spectra of HSA and its complexes with different cholesterol concentrations in the region 1800-1500 cm^{-1}.

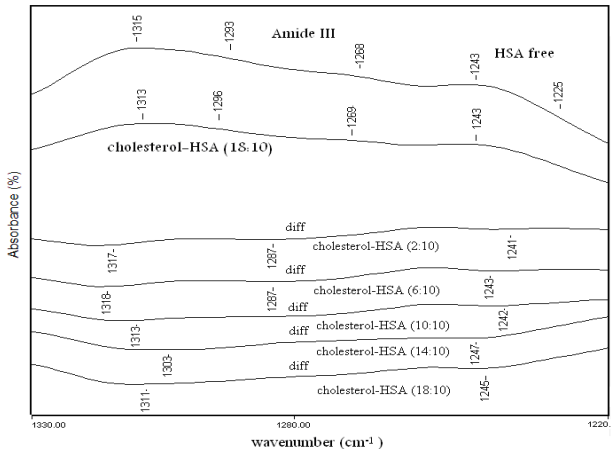

Figure 9. FT-IR spectra (top two curves) and difference spectra of HSA and its complexes with different cholesterol concentrations in the region of 1330- 1220 cm^{-1}.

1287cm^{-1} at low content of cholesterol and disappeared as the contents of cholesterol was increased (figure 9).

It is clearly shown that the strong negative features in the difference spectra became stronger as contents of cholesterol was increased with a little shift in their positions, which are attributed to the intensity decrease in the amide I, II and III bands in the spectra of the cholesterol– HSA mixtures, that is due to the interaction (H bonding) of the cholesterol with protein C=O and C-N groups, and the reduction of the proteins α-helix structure upon cholesterol–HSA interaction[51,52].

Determination of the secondary structure of HSA and its cholesterol mixtures was carried out on the basis of the procedure described by Byler and Susi[56]. In this work, a quantitative analysis of the protein secondary structure for the free HSA and cholesterol– HSA mixtures in dehydrated films is determined from the shape of Amide I, amide II and amide III bands. Infrared Fourier self-deconvolution with second derivative resolution and curve fitting procedures, were applied to increase spectral resolution and therefore to estimate the number, position and area of each component bands. The procedure was in general carried out considering only components detected by second derivatives and the half widths at half height (HWHH) for the component peaks are kept around 5cm^{-1} , the above procedure was reported in our laboratory recent publication[10,11].

The component bands of amide I, II, and III regions were assigned to a secondary structure components according to their frequency as it was obtained from the Fourier self deconvolution that have been applied to our data; for amide I band ranging from 1610 to 1700cm^{-1} assigned as follows: 1610–1624 cm^{-1} are generally attributed to β-sheet, 1625–1640 cm^{-1} to random coil, 1646–1671 cm^{-1} to α-helix, 1672–1787 cm^{-1} to turn structure, and 1689-1700cm^{-1} to β-anti-parallel. As several groups assigned the components of amid I bands in HSA, we suggest the absorption band of amid II components ranging from 1480 to 1600cm^{-1} to be assigned as follows: 1488–1504 cm^{-1} to β-sheet, 1508–1523 cm^{-1} to random coil, 1528–1560 cm^{-1} to α-helix, 1562–1585 cm^{-1} to turn structure, and 1585-1598cm^{-1} to β-anti-parallel [10,11] and as compared to amide I assignment, amid III ranging from 1220 to 1330cm^{-1} have been suggested to be assigned as follows: 1220–1256 cm^{-1} attributed to β-sheet, 1257–1285 cm^{-1} to random coil, 1287–1301 cm^{-1} to turn structure, and 1302–1329 cm^{-1} to α-helix as compared to amid I assignment. Most investigations have concentrated on Amide I band assuming higher sensitivity to the change of protein secondary structure[57]. However, it has been reported that amide II and amide III bands has high information content and could be used for prediction of proteins secondary structure[58,59,60].

Based on the above assignments, the percentages of each secondary structure of HSA were calculated by integrated areas of the component bands in amide I, amide II and amide III then summed and divided by the total area. The obtained number is taken as the proportion of the polypeptide chain in that conformation.

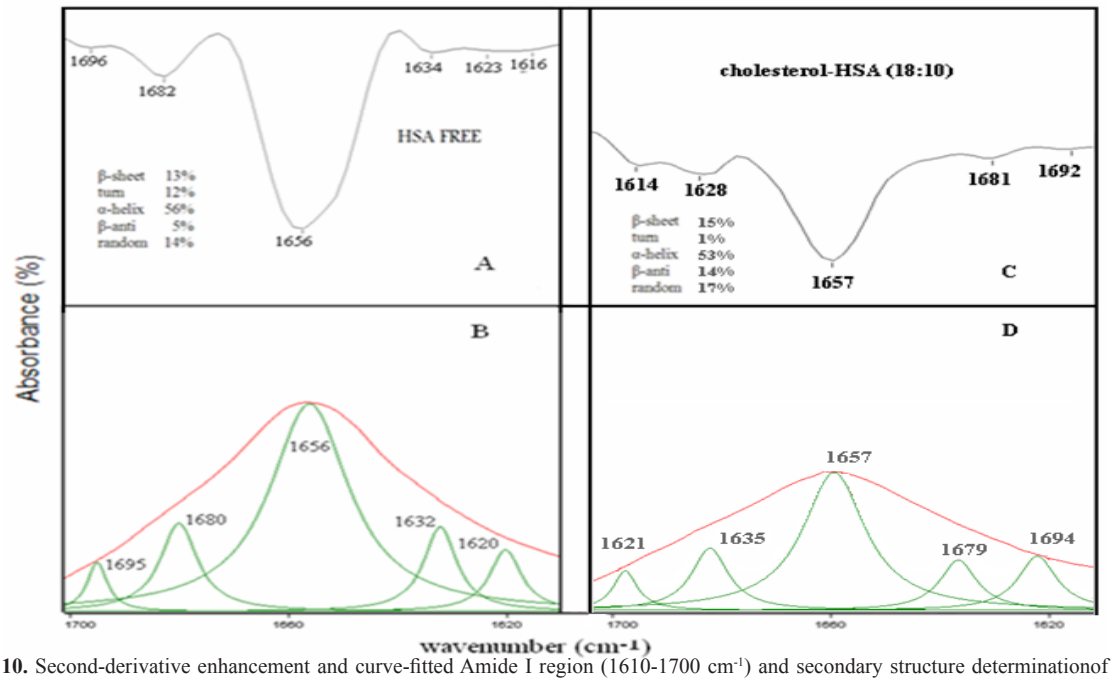

Figure 10. Second-derivative enhancement and curve-fitted Amide I region (1610-1700 cm^{-1}) and secondary structure determinationof the free human serum albumin (A and B) and it cholesterol complexes (C and D) with 18:10 cholesterol: HSA ratios.

Figure 13, Figure 14 and Figure 15 show the relative secondary structure of HSA+ Cholesterol of the anti-parallel β-sheets, the parallel β-sheets and the α-helix respectively with different molar ratio as a function of temperature. The relative percentage of the secondary structure of α-helix decreased with increasing temperature while both parallel and anti-parallel β-sheets increased with temperature. This phenomena was observed in both free HSA and HSA-cholesterol mixture. These results can be explained by the location of α-helices on the surface of HSA tertiary structure as well as the hydrogen bonding between its residues are longer than their corresponding ones in both types of β-sheets. As indicated before, this make the hydrogen bonds more susceptible to be broken by both temperature and cholesterol interactions in α-helices than hydrogen bonds in both types of β-sheets. The relative decrease in α-helices molecular content percentage cause the relative increase in β-sheets molecular content percentage in HSA tertiary structure.

The Secondary structure determination for the free HSA and its cholesterol mixtures with different drug contents are given in (Table 2). The second derivative resolution enhancement and curve – fitted Amide I, Amide II, and Amide III regions and secondary structure determinations of the free human serum albumin (A, B) and its cholesterol mixtures (C, D) with the highest contents of cholesterol in dehydrated films are shown in (Fig. 10, Fig. 11, and Fig. 12).

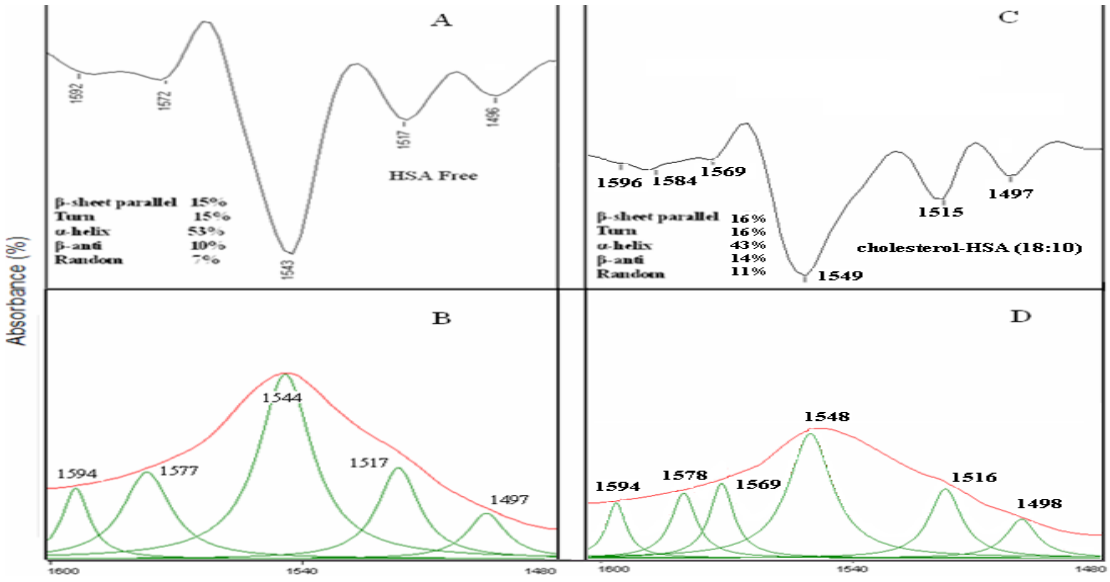

Figure 11. Second-derivative enhancement and curve-fitted Amide II region (1600-1480 cm^{-1}) and secondary structure determination of the free human serum albumin (A and B) and it cholesterol complexes (C and D) with 18:10 cholesterol: HSA ratios.

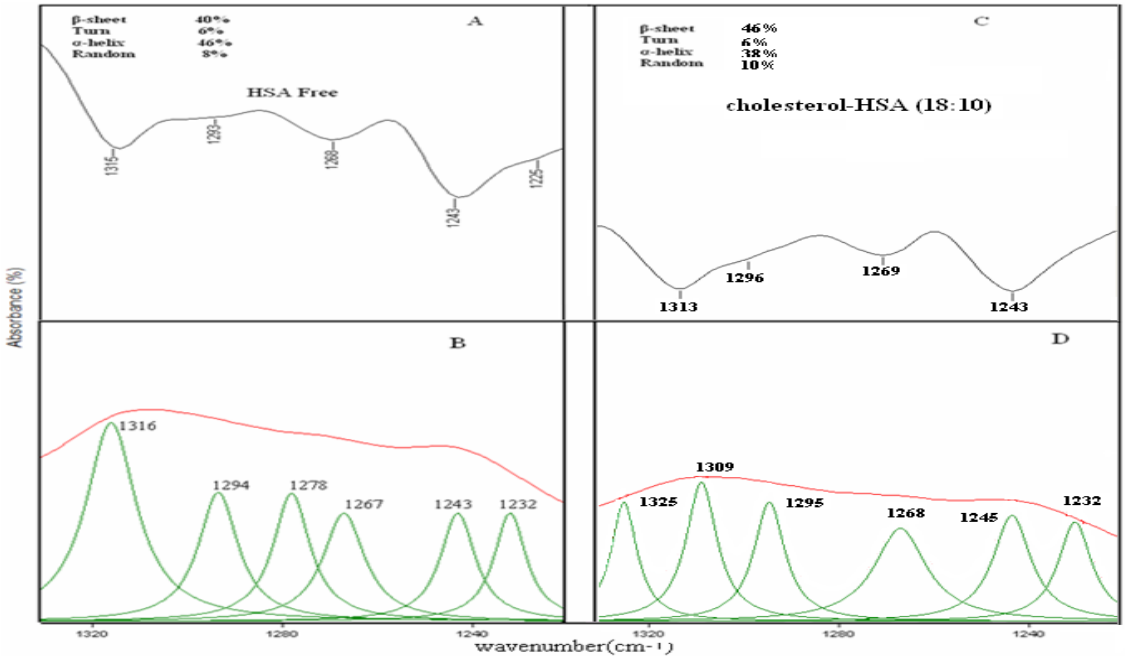

Figure 12. Second-derivative resolution enhancement and curve fitted amide III region (1330-1220 cm^{-1}) and secondary structure determination of the free human serum albumin (A,B) and its cholesterol complexes (C,D) with 18:10 cholesterol: protein ratio.

Table 2. Secondary structure determination for Amide I, amide II, and amide III regions in HSA and its Cholesterol complexes.

2nd Structure	HSA free(%)	chol -HSA 2:10(%)	chol -HSA 6:10(%)	chol -HSA 10:10(%)	chol -HSA 14:10(%)	chol -HSA 18:10(%)
Amide I						
β-sheets (cm^{-2}) (1610-1624) (1687-1700)	17	23	23	25	26	29
Random(cm^{-2}) (1625-1640)	8	4	3	2	1	1
α-hilex (cm^{-2}) (1643-1671)	57	57	57	56	55	53
Turn (cm^{-2}) (1672-1687)	18	16	17	17	18	17
Amide II						
β-sheets (cm^{-2}) (1488-1504) (1585-1598)	25	29	28	29	32	30
Random(cm^{-2}) (1508-1523)	7	12	13	12	9	11
α-hilex (cm^{-2}) (1525-1560)	53	42	42	42	41	43
Turn (cm^{-2}) (1562-1585)	15	17	17	17	18	16
Amide III						
β-sheets (cm^{-2}) (1220-1256)	40	45	47	46	45	46
Random(cm^{-2}) (1257-1285)	8	8	7	8	11	10
Turn (cm^{-2}) (1287-1301)	6	6	6	6	5	6
α-hilex (cm^{-2}) (1302-1329)	46	41	40	40	39	38

Table 2 shows the relative percentage of each secondary structure of HSA before and after the interaction with cholesterol at different cholesterol concentration. It is obviously seen that α-helix percentage decrease with the increase of cholesterol concentration and this trend is consistent in the three Amide regions.

For cholesterol- HSA interactions in amide I region free HSA consists of (57%) α-helical structure ,(17%) β-sheet, (18%) turn structure, and (8%) random coil. After cholesterol-HSA mixing, see Figure 10 and table 2, α-helical structure reduced from 57% to 53%, β-sheet increased from 17% to 29%, turn structure reduced from 18% to 17%, and the random coil reduced from 8% to 1%. In amide II region HSA free consists of (25%) β-Sheet, (7%) random coil, (53%) α-helical structure, and (15%) turn structure. After cholesterol- HSA interaction, see Figure 11 and table 2, α-helical structure reduced from 53% to 43%, β-sheet increased from 25% to 30%, turn structure reduced from 15% to 16%, and the random coil increased from 7% to 11%. And in amide III region HSA free consists of (40%) β-Sheet, (8%) random coil, (46%) α-helical structure, and (6%) turn structure. After cholesterol- HSA interaction, see Figure 12 and table 2, α-helical structure reduced from 46% to 38%, β-sheet increased from 40% to 46%, no change in the turn structure which is kept at 6%, and the random coil increased from 8% to 10%.

The reduction of α-helix intensity percentage in favor of the increase of β-sheets are believed to be due to the unfolding of the protein in the presence of cholesterol as a result of the formation of H bonding between HSA and the cholesterol. The newly formed H-bonding result in the C–N bond assuming partial double bond character due to a flow of electrons from the C=O to the C–N bond which decreases the intensity of the original vibrations[50] and the hydrogen bonds in α-helix are formed inside the helix and parallel to the helix axis, while for β-sheet the hydrogen bonds take position in the planes of β-sheets as

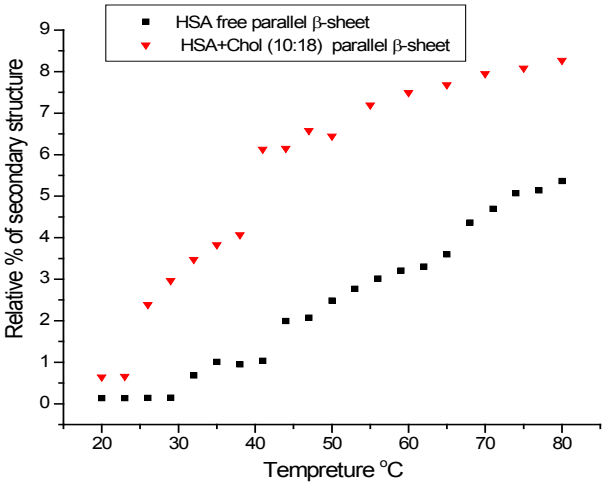

Figure 14. Relative % of secondary structure of HSA+ Cholesterol" Parallel β-sheet", different Molar ratio vs temperature. The isolated symbols on the right correspond to the respective secondary structure components.

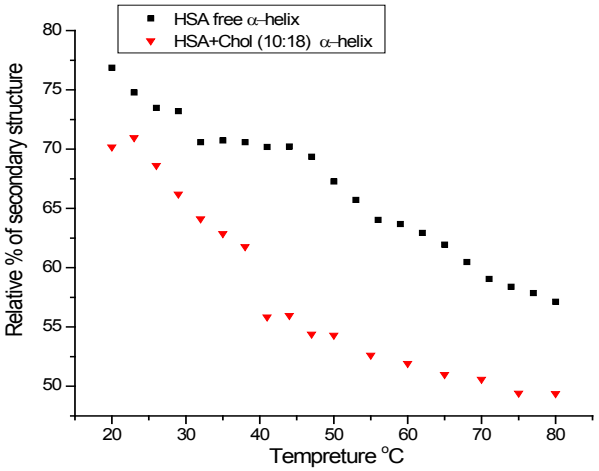

Figure 15. Relative % of secondary structure of HSA+ Cholesterol "α-helix", different Molar ratio vs temperature. The isolated symbols on the right correspond to the respective secondary structure components.

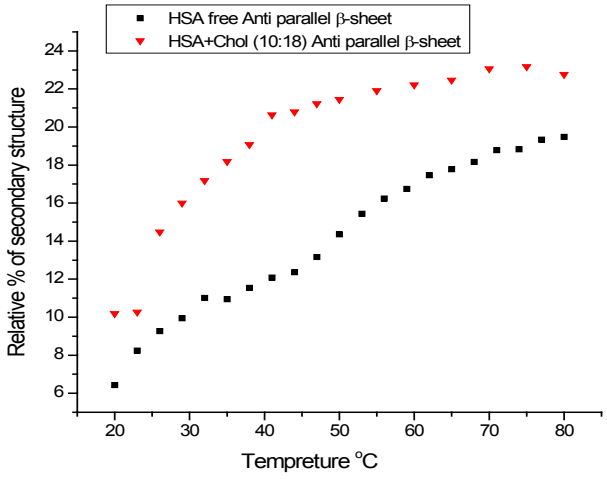

Figure 13. Relative % of secondary structure of HSA+ Cholesterol" Anti parallel β-sheet", different Molar ratio vs temperature. The isolated symbols on the right correspond to the respective secondary structure components.

the preferred orientations especially in the anti-parallel sheets, so the restrictions on the formation of hydrogen bonds between cholesterol and β-sheet relative to the case in α-helix explains the larger effect on reducing the intensity percentage of α-helix to that of β-sheet. Similar conformational transitions from an α-helix to β-sheet structure were observed for the protein unfolding upon protonation and heat denaturation[61,62].

CONCLUSION

The binding of cholesterol to HSA has been proven by UV-absorption spectroscopy, fluorescence spectroscopy and by FTIR spectroscopy. From the UV and Fluorescence Investigations we determined values for the binding constant and the quenching constant. The results indicate that the intrinsic fluorescence of HSA was quenched by cholesterol through static quenching mechanism. Analysis of the FTIR spectra reveals that HSA – cholesterol interaction results in major protein secondary structural changes in the compositions of a-helix at the advantages of the b-sheets. Reflected in the decrease of relative percentage of a-helices parallel with an increase in the relative percentage of b-sheets in HSA secondary structure composition.

Acknowledgements

This work is supported by the German Research Foundation DFG grant No. DR228/24-2

REFERENCES

[1] Hardie D G. 1991. Biochemical Messengers, Hormones, Neurotransmitters And Growth Factors, 1st, university press, Cambridge.

[2] Pani A., Dessi S., Copyright ©2003 Eurekah.com and Kluwer Academic / Plenum Publishers Cell Growth and Cholesterol Esters.

[3] F. Korkmaz, F. Severcan / Archives of Biochemistry and Biophysics 440 (2005) 141–147

[4] Maiti T K., Ghosh K S., Samanta A., Dasgupta S. 2008. The interaction of Silibinin with Human serum albumin: A spectroscopic investigation. Journal of Photochemistry and Photobiology A. 194: 297-307.

[5] Jürgens G., Müller M., Garidel P., Koch M H J., Nakakubo H., Blume A., Brandenburg K. 2002. Re-lipopolysaccharide and lipid A Investigation into the interaction of recombinant human serum albumin with. Journal of Endotoxin Research. 8: 115-126.

[6] Ouameur A A., Mangier E., Diamantoglou1 S., Carpentier R., Tajmir Riahi H A. (2004). Effects of organic and inorganic polyamine cations on the structure of human serum albumin. Biopolymers. 73:503-509.

[7] Ha J S., Theriault A., Bhagavan N V., Ha C E. 2006. Fatty acids bound to human serum albumin and its structural variants modulate apolipoprotein B secretion in HepG2 cells. Biochimica et Biophysica Acta.1761: 717-724.

[8] Tang J., Luan F., Chen, X. 2006. Binding analysis of glycyrrhetinic acid to humanserum albumin: fluorescence spectroscopy, FTIR, and molecular modeling. Bioorg. Med Chem. 14: 3210-3217.

[9] Protein & Peptide Letters, 2008, Vol. 15, No. 4 The Interaction between Cholesterol and Human Serum Albumin Liu Penga L., Minboa H., Fangb C., Xia L. and Chaocana L.

[10] Darwish S M., Abu sharkh S E., Abu Teir M M., Makharza S A., Abu hadid M M.2010. Spectroscopic investigations of pentobarbital interaction with human serum albumin. Journal of Molecular Structure. 963: 122-129.

[11] Abu Teir M M., GHITHAN S J.H., DARWISH S., ABU-HADID M.M. / Journal of Applied Biological Sciences, 5 (13): 35-47, 2011, Study of Progesteroneinteraction with Human Serum Albumin: Spectroscopic Approach.

[12] Cui F., Qin L., Zhang G., Liu X., Yao X., Lei B. 2008. A concise approach to 1,11- didechloro-6-methyl-40-O-demethyl rebeccamycin and its binding to human serum albumin: Fluorescence spectroscopy and molecular modeling method.Bioorganic and Medical Chemistry.16: 7615-7621.

[13] Kang J., Liu Y., Xie M X., Li S., Jiang M., Wang Y D. 2004. Interactions of human serum albumin with chlorogenic acid and ferulic acid. Biochimica et Biophysica Acta.1674: 205-214.

[14] Rondeau P., Armenta S., Caillens H., Chesne S., Bourdon E. 2007. Assessment of temperature effects on b-aggregation of native and glycated albumin by FTIR spectroscopy and PAGE: Relations between structural changes and antioxidant properties. Archives of Biochemistry and Biophysics. 460: 141-150.

[15] Wybranowski, T., Cyrankiewicz, M., Ziomkowska, B., Kruszewski, S. 2008. The HSA affinity of warfarin and flurbiprofen determined by fluorescence anisotropy measurements of camptothecin. BioSystems. 94:258-262.

[16] Sereikaite J., Bumelis V.A. 2006. Congo red interaction with α-proteins. Acta Biochim. Pol. 53: 87-91.

[17] Jianghong T., Ning L., Xianghong H., Guohua Z. 2008. Investigation of the interaction between sophoricoside and human serum albumin by optical spectroscopy and molecular modeling methods. J. Mol. Struct. 889: 408-414.

[18] Surewicz W K., Mantsch H H., Chapman D. 1993. Determination of protein secondary structure by Fourier transform infrared spectroscopy: A critical assessment. Biochemistry. 32: 389-394.

[19] Dukor R K., Chalmers J M., Griffiths P R. 2001. Vibrational Spectroscopy in the Detection of Cancer, Handbook of Vibrational Spectroscopy, Vol. 5, John Wiley and Sons, Chichester.

[20] Chirgadze Y N., Fedorov V., Trushina P P. 1975. Estimation of Amino Acid Residue Side-Chain Absorption in the Infrared Spectra of Protein Solutions in Heavy Water. Biopolymers. 14: 679-694.

[21] Bi S Y., Song D Q., Yian Y., Liu X Y., Zhang H Q. 2005. Molecular spectroscopic study on the interaction of tetracyclines with serum albumins. Spectochim. Acta. Part A. 61: 629-636.

[22] Peng L., Minboa H., Fang C., Xi L., Chaocan Z. 2008. The Interaction Between Cholesterol and Human Serum Albumin. Protein & Peptide Letters. 15: 360-364.

[23] Stephanos J J. 1996. Drug-Protein Interactions: Two-Site Binding of Heterocyclic Ligands to a Monomeric Hemoglobin. J. Inorg. Biochem.62: 155-169.

[24] Klotz M I., and Hunston L D. 1971. Properties of graphical representations of multiple classes of binding sites. Biochemistry. 10: 3065-3069.
[25] Lakowicz J R. 2006. Principles of Fluorescence Spectroscopy, 3rd, Springer Science+Business Media, USA.
[26] Kragh-Hansen U. 1981. Molecular aspects of ligand binding to serum albumin. Pharmacol. Rev. 33: 17-53.
[27] Purcell M., Neault J F., Tajmir-Riahi H A. 2000. Interaction of taxol with human serum albumin. Biochimica et Biophysica Acta. 1478:61-68.
[28] Neault J F., and Tajmir-Riahi H A. 1998. Interaction of cisplatin with human serum albumin. Drug binding mode and protein secondary structure. Biochimica et Biophysica Acta. 1384: 153-159.
[29] Royer C A. 1995. Approaches to Teaching Fluorescence Spectroscopy. Biophysical Journal. 68: 1191-1195.
[30] Sulkowska A. 2002. Interaction of drugs with bovine and human serum albumin. J. Mol. Struct. 614: 227-232.
[31] Tian J N., Liu J Q., Zhang J Y., Hu Z D., Chen X G. 2003. Fluorescence Studies on the Interactions of Barbaloin with Bovine Serum Albumin. Chem. Pharm. Bull. 51: 579-582.
[32] Petitpas I., Bhattacharya A A., Twine S., East M., Curry S. 2001. Crystal structure analysis of warfarin binding to human serum albumin. Journal of Biological Chemistry. 276: 22804-22809.
[33] Wang C., Wu Q., Li C., Wang Z., Ma J., Zang X., Qin N. 2007. Interaction of Tetrandrine with Human Serum Albumin: a Fluorescence Quenching Study. Analytical Sciences. 23: 429-433.
[34] Gerbanowski, A., Malabat, C., Rabiller, C., Gueguen, J. (1999). J. Agric. Food Chem. 47, p5218.
[35] Cui F., Wang J., Cui Y., Yao X., Qu G., Lu Y. 2007. Investigation of interaction between human serum albumin and N6-(2-hydroxyethyl) adenosine byfluorescence spectroscopy and molecular modelling. Luminescence. 22: 546-553.
[36] Cheng F Q., Wang Y P., Li Z P., Chuan D. 2006. Fluorescence study on the interaction of human serum albumin with bromsulphalein. Spectrochimica Acta Part A. 65: 1144-1147.
[37] Lakowica J. R., Weber G. 1973. Quenching of fluorescence by oxygen. A probe for structural fluctuations in macromolecules. Biochem. 12: 4161-4170.
[38] Eftink M.R. 1991. Fluorescence Quenching Reactions: Probing Biological Macro molecular structures. In Biophysical and Biochemical Aspects of Fluorescence Spectroscopy, Plenum, New York.
[39] Lakowicz JR, Weber G. Quenching of protein fluorescence by oxygen. Detection of structural fluctuations in proteins on the nanosecond time scale. Biochemistry. 1973 Oct 9;12(21):4171–4179.
[40] Wang T., Xiang B., Wang Y., Chen C., Dong Y., Fang H., Wang M. 2008.Spectroscopic investigation on the binding of bioactive pyridazinone derivative tohuman serum albumin and molecular modeling. Colloids Surf. B. 65: 113-119.
[41] Yang M M., Yang P., Zhang L W. 1994. Study on interaction of caffeic acid series medicine and albumin by fluorescence method. Chin. Sci. Bull., 39: 734-739.
[42] Cui F., Wang J., Li F., Fan J., Qu G., Yoa X., Lei B. 2008. Investigation of the Interaction between Adenosine and Human Serum Albumin by Fluorescent Spectroscopy and Molecular Modeling. Chinese Journal of Chemistry, 26: 661-665.
[43] Charbonneau D., Beauregard M., Tajmir-Riahi H A. 2009. Structural analysis of human serum albumin complexes with cationic lipids. J. Phys. Chem.B. 113: 1777-1784.
[43] Li Y., He W Y., Dong Y M., Sheng F., Hu Z. D. 2006. Human serum albumin interaction with formononetin studied using fluorescence anisotropy, FT-IR spectroscopy, and molecular modeling methods. Bioorganic & Medicinal Chemistry. 14: 1431-1436.
[44] Sirotkin V A., Zinatullin A N., Solomonov B N., Faizullin D A., Fedotov V D. 2001. Calorimetric and Fourier transform infrared spectroscopic study of solid proteins immersed in low water organic solvents. Biochimica et Biophysica Acta. 1547: 359-369.
[45] Arrondo J L., Muga A. 1993. Quantitative studies of the structure of proteins in solution by Fourier-transform infrared spectroscopy. Prog. Biophys. Mol. Biol. 59: 23-56.
[46] Ganim Z. and Tokmakoff A. 2006. Spectral Signatures of Heterogeneous Protein Ensembles Revealed by MD Simulations of 2DIR Spectra. Biophysical Journal. 91:2636-2646.
[47] Haris P I., and Severcan F. 1999. FTIR spectroscopic characterization of protein structure in aqueous and non-aqueous media. Journal of Molecular Catalysis B: Enzymatic. 7: 207-221.
[48] Vandenbussche G., Clercx A., Curstedt T., Johansson J., Jornvall H., Ruysschaert J M. 1992. Structure and orientation of the surfactant associated protein C in a lipidbilayer. European Journal of Biochemistry. 203: 201-209.
[49] Workman J R. 1998. Applied Spectroscopy: Optical Spectrometers, Academic Press, San Diego.
[50] Jackson, M. and Mantsch, H. H. 1991. Protein secondary structure from FT IR spectroscopy with dihedral angles from three-dimensional Ramachandran plots. J. Chem. 69: 1639-1643.
[51] Krimm S. and Bandekar J. 1986. Vibrational Spectroscopy and Conformation of Peptides, Polypeptides, and Proteins. Adv. Protein Chem. 38: 181-364.
[52] Purcell M., Neault J.F. ,Malonga H., Arakawa H., and Tajmir-RiahiCan H.A.. J. Chem. 79: 1415–1421 (2001).
[53] Fabian H., Schultz C., Backmann J., Hahn U., Saenger W., Mantsch H H., Naumann D. 1994. Impact of point mutations on the structure and thermal stability of ribonuclease T1 in aqueous solution probed by Fourier transform infrared spectroscopy. Biochemistry. 33: 10725-10730.
[54] Yamamoto T. and Tasumi M. 1991. FT-IR studies on thermal denaturation
processes of ribonucleases A and S in H2O and D2O solutions. J. Mol. Struct. 242: 235-244.
[55] Matsuura H., Hasegawa K., Miyazawa T. 1986. Infrared and Raman spectra of N-acetyl-l-amino acid methylamides with aromatic side groups. Spectrochim. Acta. 42: 1181-1192.

[56] Byler M. and Susi H. 1986. Examination of the secondary structure of proteins bydeconvolved FTIR spectra. Biopolymers. 25: 469-487.

[57] Vass E., Holly S., Majer Z., Samu J., Laczko I. Hollosi M. 1997. FTIR and CD spectroscopic detection of H-bonded folded polypeptide structures. Journal of Molecular Structure. 408/409: 47-56.

[58] Oberg K A., Ruysschaert J M., Goormaghtigh E. 2004. The optimization of protein secondary structure determination with infrared and circular dichroism spectra.Eur. J. Biochem. 271: 2937-2948.

[59] Jiang M., Xie M X., Zheng D., Liu Y., Li X Y., Chen X. 2004. Spectroscopic studies on the interaction of cinnamic acid and its hydroxyl derivatives with human serum albumin. Journal of Molecular Structure. 692: 71-80.

[60] Liu Y., Xie M X., Kang J., Zheng D. 2003. Studies on the interaction of total saponins of panax notoginseng and human serum albumin by Fourier transform infrared spectroscopy. Spectrochim. Acta. Part A. 59: 2747-2758.

[61] Surewicz W K., Moscarello M A., Mantsch H H. 1987. Secondary structure of the hydrophobic myelin protein in a lipid environment as determined by Fourier- transform infrared spectrometry. J. Biol. Chem. 262: 8598-8609.

[62] Holzbaur, I.E., English, A.M., Ismail, A.A. (1996). FTIR Study of the Thermal Denaturation of Horseradish and Cytochrome c Peroxidases in D2O. Biochemistry.35: 5488-5494.